Research Journal of Applied Sciences, Engineering and Technology 5(1): 192-202, 2013
DOI:10.19026/rjaset.5.5104
ISSN: 2040-7459; e-ISSN: 2040-7467

Submitted: May 15, 2012 Accepted: June 06, 2012 Published: January 01, 2013

Research Article

A Single Monitor Method for Voltage Sag Source Location using Hilbert Huang Transform

Wong Ling Ai and Hussain Shareef
Department of Electrical, Electronic and System Engineering, UKM, Bandar Baru Bangi, Malaysia

Abstract: This study introduces a method for voltage sag source location based on Hilbert Huang transformed monitored current signal. Unlike the traditional method, the proposed method first transforms the recorded current during the sag event to obtain frequency-time plot (Hilbert spectra) and IMF plot before the location of voltage sag source is determined. Then based on the change in frequency and IMF the relative location of voltage sag source is obtained. The effectiveness of the proposed method has been verified through simulation on 20 bus system and by comparing with an existing S-Transform based method. The results show that the presented method can determine the location of voltage sag source correctly.

Keywords: Hilbert Huang transform, power quality, signal processing, voltage sags

INTRODUCTION

Electrical Power Quality (PQ) is defined as the degree to which both utilization and delivering of electrical power affect the performance of user equipment (Mohammadi and Akbari Nasab, 2011). Most of the PQ problems are caused by power quality disturbances such as harmonics, voltage swell, voltage sag, transients, interruption, notching and etc. Among these disturbances, voltage sag is considered as the most frequent and detrimental PQ event. Heavy losses are imposed on voltage sag victim due to the damage or disoperation of the loads and equipment. This brings out the importance issue for to locate the voltage sag source because the party that generates the sag should take full responsibility on the losses due to the sag. The location of the voltage sag source also enables the service restoration to be performed quickly.

Various researches had been done to determine the voltage sag source location. One of the first works applied the concept of disturbance power and energy (Parsons *et al*., 2000). This method states that the key indicator to know the location of the disturbance source is the direction of energy flow through the network. Another method proposed the use of the slope of system trajectory (Li *et al*., 2003) where it is based on the relationships between the product of voltage magnitude and power factor and also the current magnitude where these relationships will give different measurement for different fault locations. Slightly different from two methods above, Pradhan and Routray (2005) suggested a distance relay method which locates the voltage sag source by computing the seen impedance from the estimated voltage and current phasors at the monitored location. Besides that, Tayjasanant *et al*. (2005) had proposed another method by estimating the equivalent impedance of the non-disturbance side by using the changes of voltage and current caused by the fault. Meanwhile, Ahn *et al*. (2005) proposed to detect the sag source by investigating the cause for the sag in order to decide the relative location of the sag by using the relation between them. Another approach in detecting the sag source location is based upon the magnitude of voltages obtained at both sides of the transformer that interconnects two grids and comparing the voltage sag magnitudes in per unit with the pre-fault voltages at both sides of the transformer (Leborgne and Karlsson, 2008). Meanwhile, Faisal *et al*. (2010) presented a method to detect the voltage sag sources by using a signal processing technique known as S-Transform (ST).

As mentioned in Leborgne *et al*. (2006), all phasor based methods mentioned above might have limited validity for sag disturbance location caused by asymmetrical faults generated in meshed grids. Furthermore, since the voltage sags are short duration disturbance events, all phasor-based methods might produce questionable results due to the inherent averaging in the harmonic analysis of the input signals (Polajžer *et al*., 2009).

Voltage sag event always contains high frequency component. In order to avoid problems faced by phasor-based methods, the instantaneous frequency variations

Corresponding Author: Wong Ling Ai, Department of Electrical, Electronic and System Engineering, UKM, Bandar Baru Bangi, Malaysia

can be used in voltage sag source detection by using some techniques. This study introduces Hilbert Huang Transform (HHT) (Huang, 2005) based method for accurate detection of voltage sags. The current signals are transformed into a new view of frequency-time plot (Hilbert spectra) and Intrinsic Mode Function (IMF) plot and the location of the fault in the system is determined by the analysis of the waveform shown in the plots.

The study is structured as follows. The basic principle of the HHT is presented next, followed by a brief explanation of HHT based method in sag source location. Then, results from HHT using simulation data are provided and discussed. Lastly, the conclusions are drawn.

THE HILBERT HUANG TRANSFORM (HHT)

This section introduces the basic concept of HHT. Frequency analysis is the second most important method in signal processing after the time analysis method. For the frequency analysis, the Fourier analysis has played an important role in stationary signal analysis since year 1807 (Cohen, 1995). However, there are some limitations on Fourier analysis since it can be only applied on linear system with stationary data. Therefore, HHT is introduced in this study since it provides physically meaningful representations of data for non-stationary and non linear processes, especially for time-frequency-energy representations (Huang, 2005). It is a data analysis method which is empirically-based and it is mainly make up of two parts, Empirical Mode Decomposition (EMD) and Hilbert Spectra Analysis (HSA). Let's examine a simple non linear system as given by the non-dissipative Duffing equation as:

$$\frac{d^2x}{dt^2} + x(1+\varepsilon x^2) = \gamma\cos(\omega t) \tag{1}$$

where, ε is a parameter not necessarily small and γ is the amplitude of a periodic forcing function with a frequency ω. The quantity within the parenthesis can be treated as a variable spring constant and the system given in (1) should change in frequency from location to location and time to time, even within one cycle of oscillation.

The easiest way to calculate the instantaneous frequency is by using the HHT where the complex conjugate y (t) of any real valued function x (t) of Lp class can be determined by:

$$H[x(t)] = \frac{1}{\pi} PV \int_{-\infty}^{\infty} \frac{x(\tau)}{t-\tau} d\tau \tag{2}$$

where, the PV indicates the principle value of the single integral. In HHT, the analytic signal is defined as:

$$z(t) = x(t) + iy(t) = a(t)e^{i\theta(t)} \tag{3}$$

where,

$$a(t) = \sqrt{x^2 + y^2} \tag{4}$$

$$\theta(t) = \arctan(\frac{y}{x}) \tag{5}$$

while, a (t) is the instantaneous amplitude and θ (t) is the phase function and the instantaneous frequency, ω is just simply:

$$\omega = \frac{d\theta}{dt} \tag{6}$$

The instantaneous frequency can also be used in the determination of voltage sag source location. The location of the fault in the system was determined by the analysis of the waveform shown in the plots and determining a suitable index. The examples of frequency-time plot and IMF plot for the phase current that caused the voltage sag are shown in Fig. 1.

HHT based method for voltage sag source detection: The sag source location is identified based on single monitor concept as illustrated in Fig. 2 where it determined the location as upstream or downstream sag. Upstream is usually make up of power source which supply the power and downstream is usually the receiving end of the power. In the case of upstream and downstream concept, when a fault occurs at upstream, current flows to the downstream will decrease while on the other hand, when a fault occurs at downstream, most of the current will flow to the downstream.

In this research, phase current for faulty phase recorded by the monitor was used as a monitoring parameter. The HHT disturbance current is defined as:

$$\Delta I_{hht}(t) = I_{hht}(t)_{sag} - I_{hht}(t)_{presag} \begin{cases} <0 & \text{upstream} \\ >0 & \text{downstrean} \end{cases} \tag{7}$$

where, $I_{hht}(t)_{sag}$ and $I_{hht}(t)_{presag}$ are the instantaneous HHT time-frequency representing current during sag and steady state respectively in frequency-time plot.

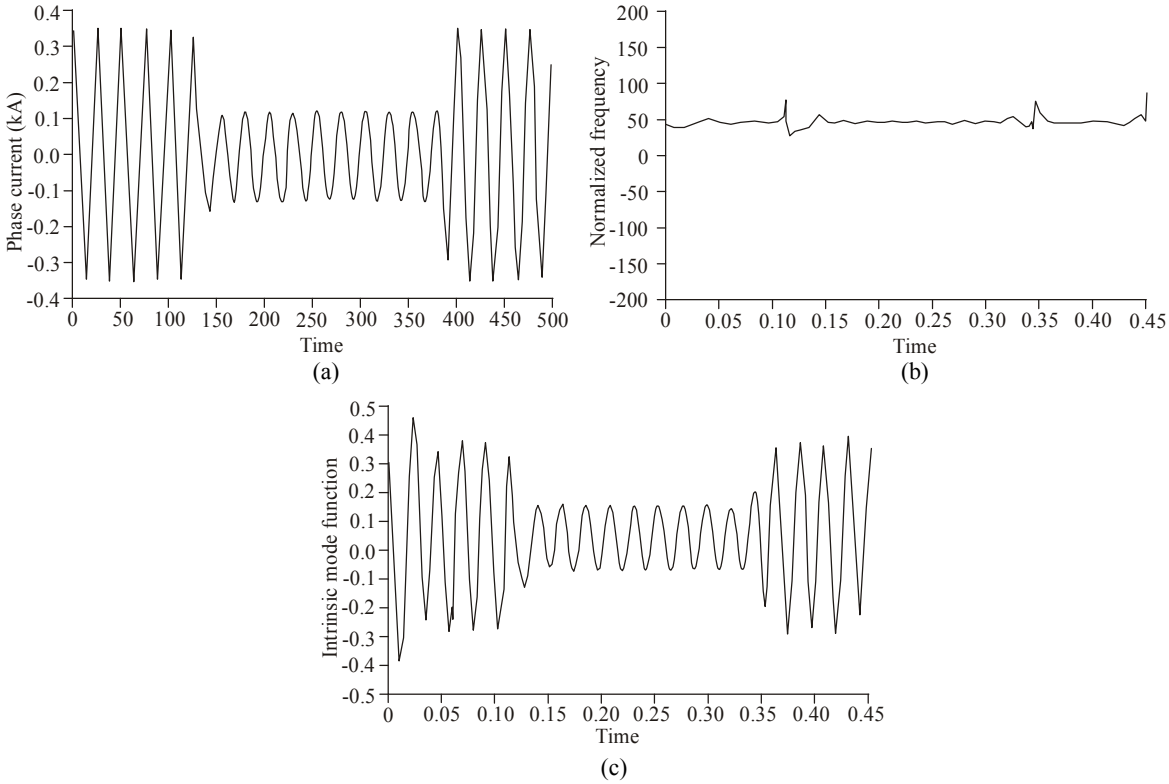

Fig. 1: Waveforms for (a) actual current signal, (b) frequency-time plot of current signal, (c) IMF plot of current signal

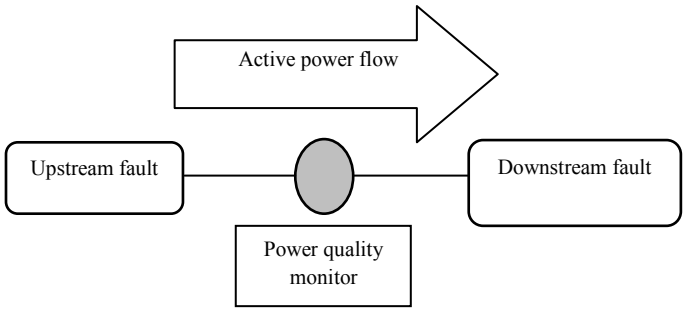

Fig. 2: Concept to determine upstream and downstream sags

Similarly, the waveform presented by IMF plot was analyzed by observing the magnitude, M_{IMF} of the waveform. As shown in (8), M_{IMF} decreases during the fault for upstream case and increases during the fault for downstream case:

$$\Delta M_{IMF} = M_{IMFsag} - M_{IMFpresag} \begin{cases} <0 & \text{upstrean} \\ >0 & \text{downstrea} \end{cases} \quad (8)$$

where, M_{IMFsag} and $M_{IMFpresag}$ are the magnitude of the IMF waveform during sag and steady state respectively.

RESULTS AND DISCUSSION

In this section simulation results of the proposed methods for voltage sag source location are presented. A 20 bus system as shown in Fig. 3 with 33 kV, 15 MVA source at 50 Hz frequency was modelled. The system

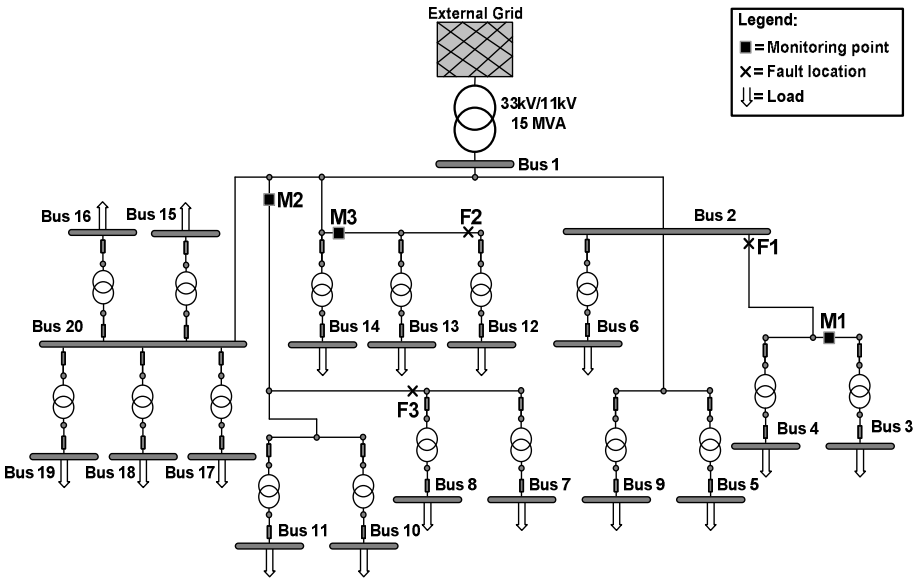

Fig. 3: Simulated test system for voltage sag source detection

has four main feeders where each feeder is connected to different numbers of step down transformers according to the load sizes.

In this study, three Power Quality Monitors (PQM) which are M1, M2 and M3, respectively were placed in the 20 bus system. Three fault points, F1, F2 and F3 were located in the system as well. The system was then simulated for different types of short circuits tests and load flow analysis. The faults created in short circuit tests include both balanced fault and unbalanced faults. The instantaneous waveforms from the monitors were obtained after the simulation.

Results of simulated system: The simulation results are generally divided into two sections according to the types of faults, which are unbalanced fault and balanced fault. Single Line to Ground fault (SLG) and Double Line to Ground fault (DLG) are grouped as unbalanced fault while three phase fault is the balanced fault. The locations of the each fault relatively to the monitors for both types of faults are shown in the Table 1. Results obtained through an existing method which used S Transform (ST) (Faisal *et al*., 2010) are also presented for comparison purpose. When there is upstream sag, the S Transform Disturbance Power (STDP) will decrease to a value lower than the presag value and vice versa for downstream sag.

Balanced voltage sags: Balanced voltage sag which is created by three phase fault (LLL fault) is first

Table 1: Relative location of the faults for each PQM

	Relative location of faults to the monitors	
Fault location	Upstream	Downstream
F1	M1, M2, M3	-
F2	M1, M2	M3
F3	M1, M3	M2

simulated. The results are presented and analyzed. Figure 4 shows the locus of various parameters plotted against time for a fault at F1. Measurement was made at M1 with the recorded instantaneous three phase voltages and currents. From Fig. 4c-e, it can be seen that the magnitude for both STDP and IMF (Intrinsic Mode Function) settle out to a value lower than the presag value from the beginning of the sag, while for the HHT ΔI_{hht} method, it starts with a peak at the beginning of the sag and then decrease to a value which is lower than the presage value before it rise back again. The characteristics shown by all three waveforms indicate that the voltage sag source is located upstream to the monitor M1.

Similarly, Fig. 5 and 6 illustrate the plots for fault at F1 measured by M2 and M3, respectively. From both figures, it can be obviously concluded that the voltage sag at F1 are located upstream to M2 and M3.

Figure 7-9 show the plots of each parameter for 3 phase fault at F2 with measurement taken at M1, M2 and M3, respectively. In Fig. 7 and 8, it can be seen that both the magnitude for STDP and IMF settle out to a value lower than the presag value during the sag while

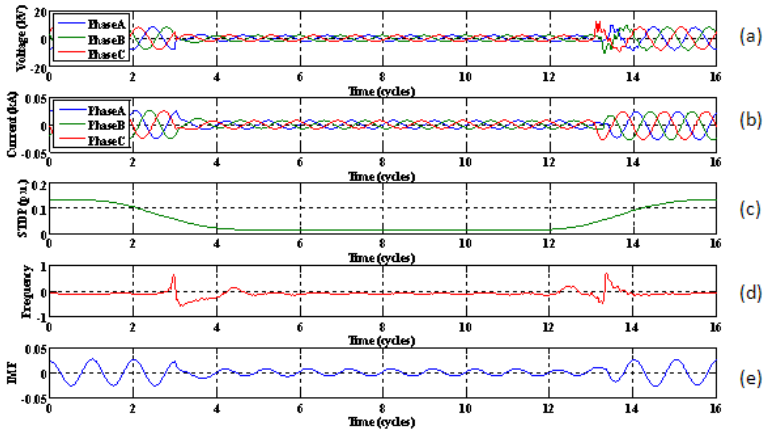

Fig. 4: Variations of STDP, frequency and IMF at M1 for LLL fault at F1: (a) voltage, (b) current, (c) STDP, (d) frequency, (e) IMF

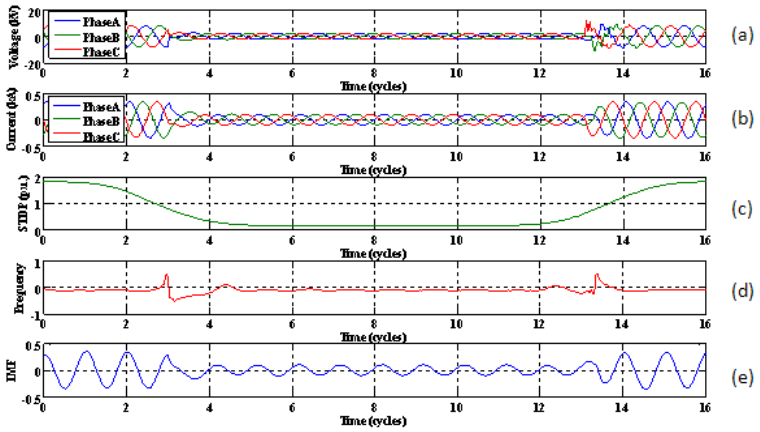

Fig. 5: Variations of STDP, frequency and IMF at M2 for LLL fault at F1: (a) voltage, (b) current, (c) STDP, (d) frequency, (e) IMF

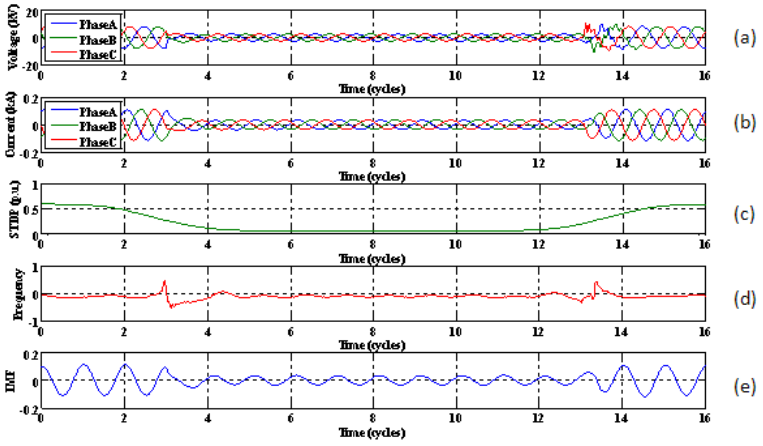

Fig. 6: Variations of STDP, frequency and IMF at M3 for LLL fault at F1: (a) voltage, (b) current, (c) STDP, (d) frequency, (e) IMF

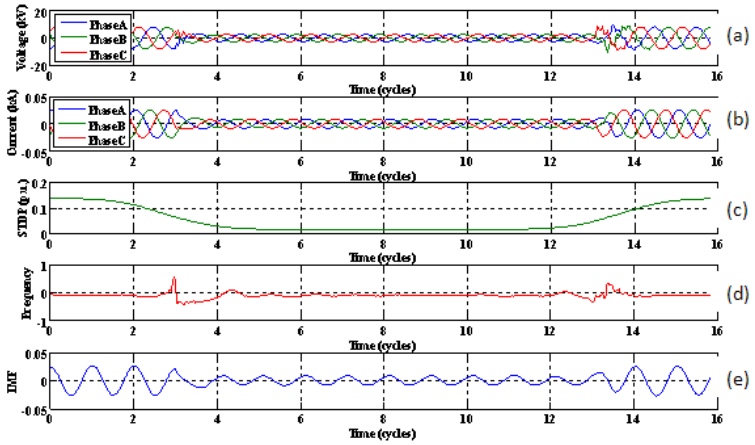

Fig. 7: Variations of STDP, frequency and IMF at M1 for LLL fault at F2: (a) voltage, (b) current, (c) STDP, (d) frequency, (e) IMF

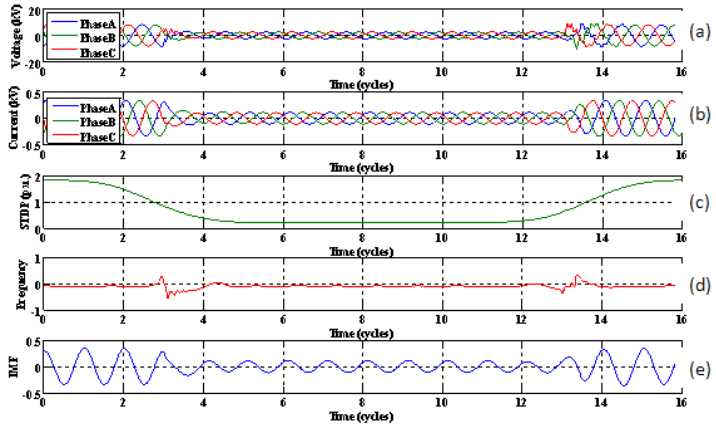

Fig. 8: Variations of STDP, frequency and IMF at M2 for LLL fault at F2: (a) voltage, (b) current, (c) STDP, (d) frequency, (e) IMF

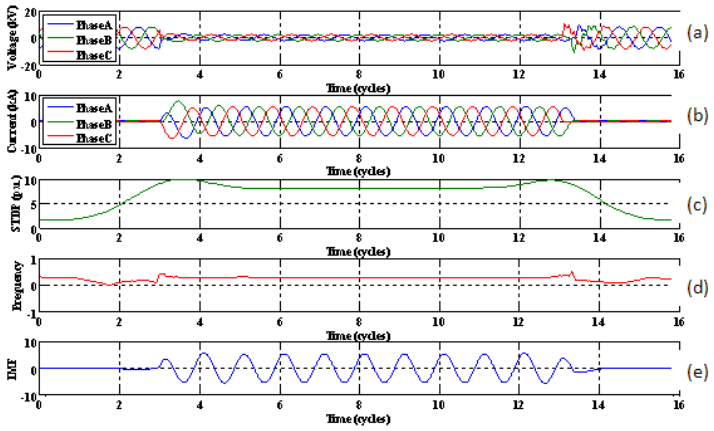

Fig. 9: Variations of STDP, frequency and IMF at M3 for LLL fault at F2: (a) voltage, (b) current, (c) STDP, (d) frequency, (e) IMF

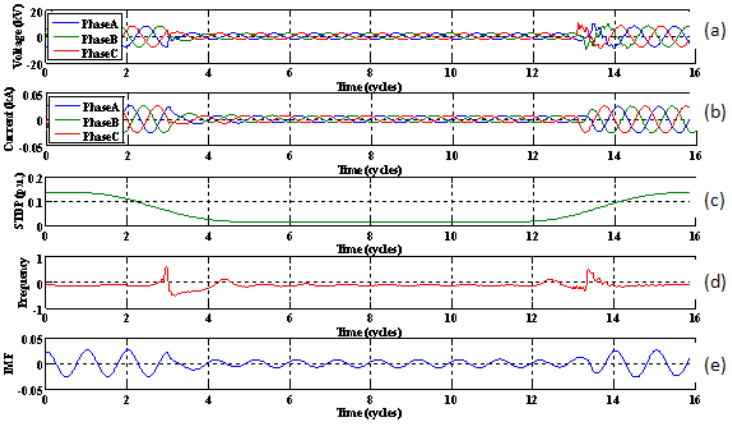

Fig. 10: Variations of STDP, frequency and IMF at M1 for LLL fault at F3: (a) voltage, b) current, (c) STDP, (d) frequency, (e) IMF

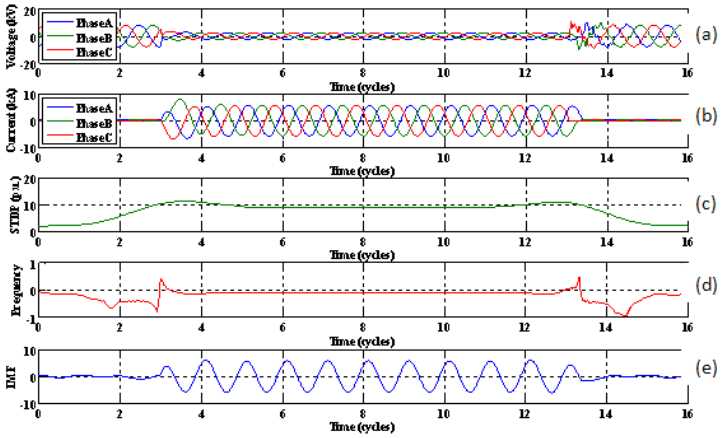

Fig. 11: Variations of STDP, frequency and IMF at M2 for LLL fault at F3: (a) voltage, (b) current, (c) STDP, (d) frequency, (e) IMF

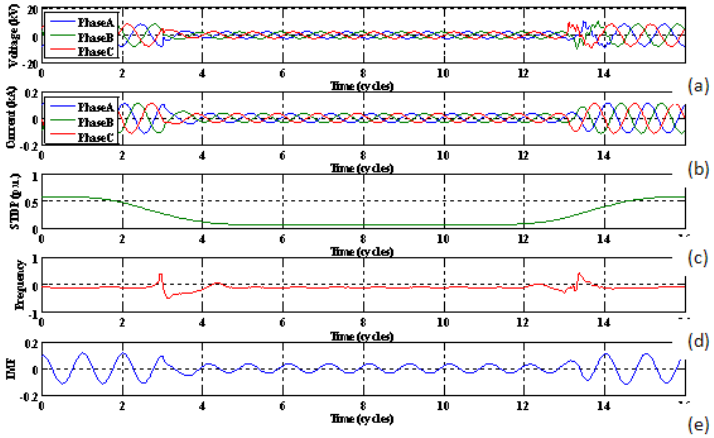

Fig. 12: Variations of STDP, frequency and IMF at M3 for LLL fault at F3: (a) voltage, (b) current, (c) STDP, (d) frequency, (e) IMF

for the HHT ΔI_{hht} frequency, the magnitude decreases after the peak which indicates the beginning of the sag. Again, these characteristics indicate that the fault F2 locates upstream to the monitors M1 and M2. On the other hand, in Fig. 9, the waveforms for Fig. 9c and 9e settle out to a value higher than the presag value during the sag and similarly for Fig. 9d, it shows an increase in frequency at the beginning of the sag, which indicates downstream voltage sag for the measurement taken at monitor M3. From the current waveforms for each figure from Fig. 7-9, one can see that the magnitude of the current increases during the downstream sag period while it decreases during the upstream sag period. This causes the values of the STDP, frequency and IMF to increase or decrease during the downstream and upstream sag event respectively.

Similarly, Fig. 10-12 show the plots for a fault at F3 where the measurements were made at monitors M1, M2 and M3, respectively. From the figures shown, it is clearly seen that the fault at F3 is upstream to the monitors M1 and M3 while downstream to monitor M2.

Unbalanced voltage sags: Other than the balanced fault, unbalanced voltage sag source is located using the proposed method as well. For the illustration purpose, two types of fault are created at F2 and the results are presented and analyzed. Table 2 shows the types of fault created at F2 and the corresponding sag location that must be recorded by monitors M1, M2 and M3.

Figure 13 shows the voltage and current waveforms at M1 and the variations of STDP, HHT ΔI_{hht} frequency and IMF due to SLG fault. From Fig. 13c-e, it can be seen that STDP and IMF all settle out to a value lower than the presag value during the sag while the HHT ΔI_{hht} frequency decreases after the peak which indicates the beginning of the sag to a value lower than presage value. Similar with the balanced fault analysis, this indicates the upstream sag to the monitor M1. In Fig. 14, the waveforms show similar pattern as in Fig. 13 which also indicates that the location of the sag is upstream to the monitor M2.

On the other hand, Fig. 15 depicts a downstream event for the monitor M3. Figure 15c-e show that both STDP and IMF settle out to a value higher than the presag value during the sag while the HHT ΔI_{hht} frequency increases at the beginning of the sag to a value higher than the presage value. Again, the magnitude of the current which increases and decreases during downstream and upstream event respectively can be observed from each figure.

Table 2: Relative sag source location to each monitor for unbalanced faults created at F2

	Relative location of faults to the monitors	
Types of fault	Upstream	Downstream
Single Line to Ground (SLG)	M1, M2	M3
Double Line to Ground (DLG)	M1, M2	M3

A double line to ground fault for phase A and phase B is simulated at F2. The voltage and current waveforms at M1 and the variations of STDP, frequency and IMF due to DLG fault are illustrated in Fig. 16. From Fig. 16c-e, it can be seen that both STDP and IMF settle out to a value lower than the presag value from the beginning of the sag while the HHT ΔI_{hht} frequency decreases to a value lower than the presage value after the peak that indicates the start of the sag. With the same concept, the sag source is known to be located upstream from the monitor M1.

Similarly, the STDP, frequency and IMF monitored by monitors M2 and M3 are shown in Fig. 17 and 18, respectively. From Fig. 17c-e, it can be seen that again, all three STDP, HHT ΔIhht frequency and IMF settle out to a value lower than the presag value from the beginning of the sag. On the contrary, Fig. 18c-e shows that all three STDP, frequency and IMF settle out to a value higher than the presag value from the beginning of the sag which indicates downstream sag from the monitor M3.

Comparing the results obtained from ST (STDP plot) and HHT (frequency plot and IMF plot) for both balanced and unbalanced faults, it is proven that the results are in agreement where all three plots correctly locate the voltage sag source. However, there is a disadvantage of S transform based method where it changes the sign far before the beginning of the sag even though there is no other type of disturbance in the raw signals. This causes the difficulty of identifying the starting and ending points of sag event. For the case of HHT based method, frequency-time plot indicates more clearly for the sag duration with its signature peaks at the beginning and end of the sag. While for the IMF plot, it changes the magnitude during sag at the same time with frequency-time plot. Simulation results show that the presented method can indicate the location of the voltage sag sources correctly.

CONCLUSION

This study has presented a new method for voltage-sag source detection which based on well known HHT signal processing technique. This method was

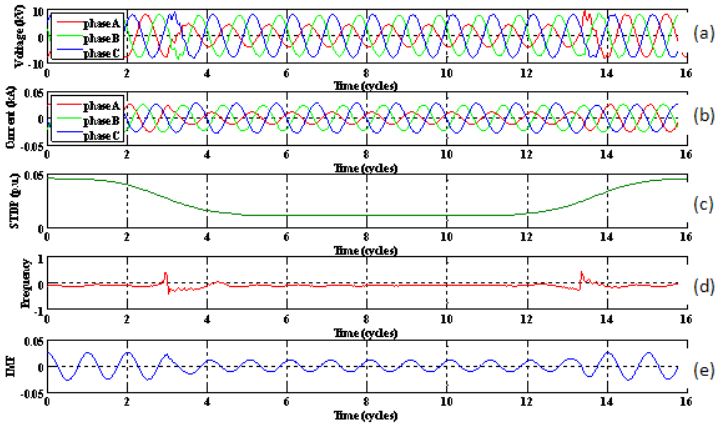

Fig. 13: Variations of STDP, frequency and IMF at M1 for SLG fault at F2: (a) voltage, (b) current, (c) STDP, (d) frequency, (e) IMF

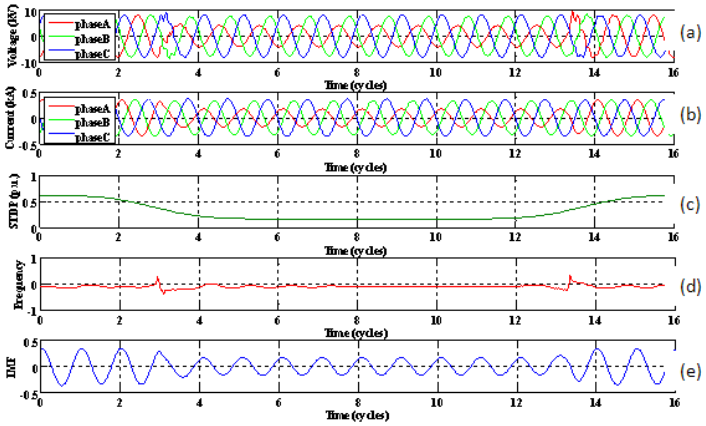

Fig. 14: Variations of STDP, frequency and IMF at M2 for SLG fault at F2: (a) voltage, (b) current, (c) STDP, (d) frequency, (e) IMF

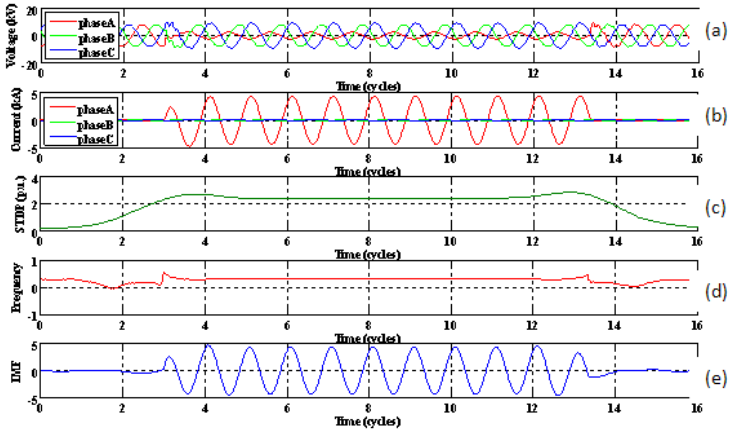

Fig. 15: Variations of STDP, frequency and IMF at M3 for SLG fault at F2: (a) voltage, (b) current, (c) STDP, (d) frequency, (e) IMF

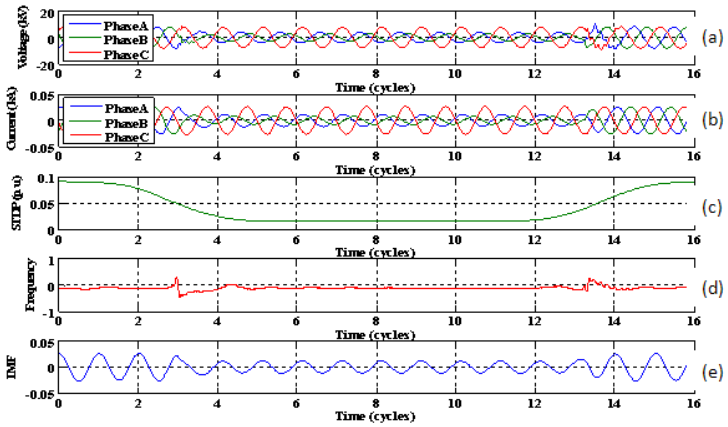

Fig. 16: Variations of STDP, frequency and IMF at M1 for DLG fault at F2: (a) voltage, (b) current, (c) STDP, (d) frequency, (e) IMF

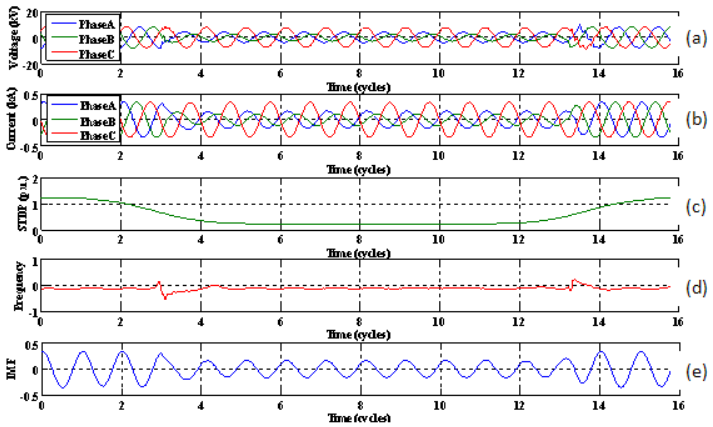

Fig. 17: Variations of STDP, frequency and IMF at M2 for DLG fault at F2: (a) voltage, (b) current, (c) STDP, (d) frequency, (e) IMF

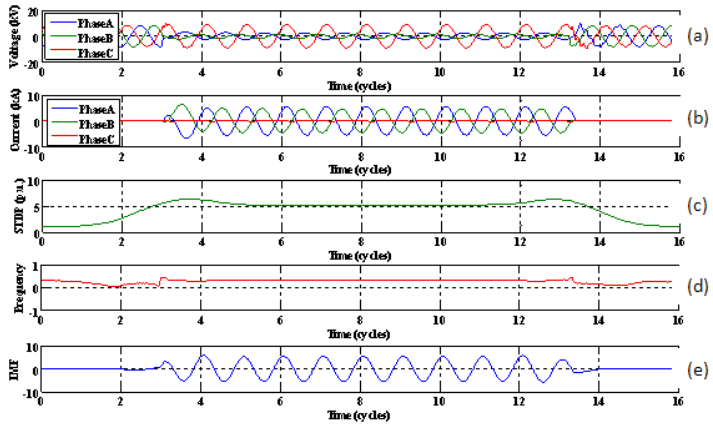

Fig. 18: Variations of STDP, frequency and IMF at M3 for DLG fault at F2: (a) voltage, (b) current, (c) STDP, (d) frequency, (e) IMF

extensively tested with numerical simulations on a 20 bus test system. Based on the performed analysis, it can be concluded that the proposed HHT based method has higher effectiveness and accuracy in detecting voltage sag source location compared to that of traditional disturbance power method.

REFERENCES

Ahn, S.J., D.J. Won, I.Y. Chung and S.I. Moon, 2005. A method to determine the relative location of voltage sag source for power quality diagnosis. Proceedings of the 16th IFAC World Congress, 16(1): 6.

Cohen, L., 1995. Time-Frequency Analysis: Theory and Applications. Prentice-Hall, Inc., New Jersey.

Faisal, M.F., M. Azah and S. Hussain, 2010. A novel voltage sag source detection method using TFR technique. Int. Rev. Elec. Eng., 5: 2301-2309.

Huang, N.E., 2005. Introduction to the Hilbert-Huang transform and its related mathematical problems. Interd. Math. Sci., 5: 1-26.

Leborgne, R.C., D. Karlsson and J. Daalder, 2006. Voltage sag source location methods performance under symmetrical and asymmetrical fault conditions. IEEE PES Transmission and Distribution Conference and Exposition Latin America, pp: 1-6.

Leborgne, R.C. and D. Karlsson, 2008. Voltage sag source location based on voltage measurements only. Electr. Pow. Qual. Utilisat. J., 14(1): 6.

Li, C., T. Tayjasanant, W. Xu and X. Liu, 2003. Method for voltage-sag-source detection by investigating slope of the system trajectory. IEE P-Gener. Transm. D., 150(3): 367-372.

Mohammadi, M. and M. Akbari Nasab, 2011. Voltage sag mitigation with D-STATCOM in distribution systems. Aust. J. Basic Appl. Sci., 5(5): 201-207.

Parsons, A.C., W.M. Grady, E.J. Powers and J.C. Soward, 2000. A direction finder for power quality disturbances based upon disturbance power and energy. IEEE T. Power Deliver., 15(3): 1081-1086.

Polajžer, B., G. Štumberger, S. Seme and D. Dolinar, 2009. Generalization of methods for voltage-sag source detection using vector-space approach. IEEE T. Ind. Appl., 45(6): 2152-2161.

Pradhan, A.K. and A. Routray, 2005. Applying distance relay for voltage sag source detection. IEEE Trans. Pow. Deliver., 20(1): 529-531.

Tayjasanant, T., L. Chun and W. Xu, 2005. A resistance sign-based method for voltage sag source detection. IEEE Trans. Pow. Deliver., 20(4): 2544-2551.